



ISSN: 1813-162X (Print); 2312-7589 (Online)

Tikrit Journal of Engineering Sciences

available online at: <http://www.tj-es.com>
**TJES**  
 Tikrit Journal of  
 Engineering Sciences

# Design, Fabrication, and Experimental Analysis of a PV Panel for a Smart Sunflower System

 Hayder A. Alnaieli <sup>a\*</sup>, Abdullateef A. Jadallah <sup>b</sup>, Ali H. Numan <sup>c</sup>
<sup>a</sup> Electromechanical Engineering Department, University of Technology, Baghdad, Iraq.<sup>b</sup> Mechanical Department, College of Engineering- Al Shirqat, Tikrit University, Tikrit, Iraq.<sup>c</sup> Electromechanical Engineering Department, University of Technology, Baghdad, Iraq.

## Keywords:

MATLAB; Photovoltaic; Smartflower; Solar; Urban.

## Highlights:

- **Smartflower:** Compact, and innovative PV system.
- **Versatile Performance:** Smartflower excels in diverse atmospheric conditions.
- **Radiant Efficiency:** More radiation, elevating power production.
- **Temperature Impact:** its rise causes power reduction of PV system.

## ARTICLE INFO


### Article history:

Received	16 June	2023
Received in revised form	16 Aug.	2023
Accepted	22 Sep.	2023
Final Proofreading	15 Dec.	2023
Available online	18 Feb.	2024

 © THIS IS AN OPEN ACCESS ARTICLE UNDER THE CC BY LICENSE. <http://creativecommons.org/licenses/by/4.0/>


**Citation:** Alnaieli HA, Jadallah AA, Numan AH. Design, Fabrication, and Experimental Analysis of a PV Panel for a Smart Sunflower System. *Tikrit Journal of Engineering Sciences* 2024; 31(1): 113-126. <http://doi.org/10.25130/tjes.31.1.10>

### \*Corresponding author:

 Hayder A. Alnaieli 

Electromechanical Engineering Department, University of Technology, Baghdad, Iraq.

**Abstract:** The Smartflower, an innovative compact energy-generation system inspired by sunflowers, stands out in energy innovation. Unlike traditional photovoltaic (PV) panels, it integrates foldable solar cells within a foundational structure for solar tracking aligned with the sun's path. The present paper focuses on designing, fabricating, and analyzing a proposed Smartflower-PV panel solar system. The study aims to comprehensively evaluate the performance of the proposed PV panel under different atmospheric conditions. The significant impact of insolation and temperature on the panel's efficiency was revealed by comparing empirical results from the PV sunflower panel with analytical calculations using MATLAB (m. file code). Enhanced solar radiation improved the system's performance and efficiency, resulting in higher power output. Analytical insights showed a direct correlation between a 104% increase in solar radiation and parallel increases of 115% in peak power production and 100% in output current. Conversely, higher temperatures reduced power output, with a 400% temperature rise causing an 11.11% power reduction. Empirical observations align with analytical analyses under equivalent conditions, validating the model's accuracy. This study serves as a catalyst and guide for completing and advancing the Smartflower system's manufacturing, including control, tracking, and the entire energy-generation framework.

# تصميم وتصنيع وتحليل تجريبي للوحة الكهروضوئية لنظام زهرة الشمس الذكي

حيدر عبد الكاظم فرحان النايي<sup>١</sup>، عبد اللطيف احمد جاد الله<sup>٢</sup>، علي حسين نعمان<sup>٢</sup>

<sup>١</sup> قسم الهندسة الكهروميكانيكية / الجامعة التكنولوجية/بغداد - العراق.

<sup>٢</sup> قسم الهندسة الميكانيكية/ كلية الهندسة - الشرقاط / جامعة تكريت / تكريت - العراق.

## الخلاصة

زهرة الشمس الذكية، نظام مبتكر لتوليد الطاقة مدمج مستوحى من زهرة الشمس حيث تدمج الخلايا الشمسية القابلة للطي ضمن هيكل أساسي لتتبع الطاقة الشمسية المتوافقة مع مسار الشمس. تركز هذه الورقة على تصميم وتصنيع وتحليل لوحة الكهروضوئية المقترحة لنظام Smartflower الشمسي. تهدف الدراسة إلى إجراء تقييم شامل لأداء الألواح الكهروضوئية المقترحة في مختلف الظروف الجوية. من خلال مقارنة النتائج التجريبية من لوحة عباد الشمس الكهروضوئية مع الحسابات التحليلية باستخدام MATLAB (m.file code)، تتم دراسة التأثير الكبير للشمس ودرجة الحرارة على كفاءة اللوحة. يؤدي تعزيز الإشعاع الشمسي إلى تحسين الأداء والكفاءة، مما يؤدي إلى زيادة إنتاج الطاقة. تُظهر الرؤى التحليلية ارتباطاً مباشراً بين زيادة الإشعاع الشمسي بنسبة ١٠٤٪ والزيادات الموازية بنسبة ١١٥٪ في ذروة إنتاج الطاقة و١٠٠٪ في تيار الخرج. على العكس من ذلك، تؤدي درجات الحرارة المرتفعة إلى انخفاض إنتاج الطاقة، مع ارتفاع درجة الحرارة بنسبة ٤٠٠٪ مما يؤدي إلى تقليل الطاقة بنسبة ١١,١١٪. تتوافق الملاحظات التجريبية مع التحليلات التحليلية في ظل ظروف معادلة، للتحقق من دقة النموذج. تعمل هذه الدراسة كمحفز ودليل لاستكمال وتطوير تصنيع نظام Smartflower، بما في ذلك التحكم والتتبع وإطار توليد الطاقة بالكامل.

**الكلمات الدالة:** ماتلاب، الخلايا الكهروضوئية، الزهرة الذكية، الطاقة الشمسية، التخطيط الحضري.

## 1. INTRODUCTION

The global energy sector faces escalating demands due to population growth and technological advances. Conventional energy sources, such as oil, natural gas, and coal, carry substantial climate impacts [1]. Consequently, the international community actively explores renewable energy sources to address energy needs. Renewable energy has gained recognition for its abundance and environmental benefits in electricity generation [2], with solar energy emerging as the foremost worldwide [3]. Growing support for photovoltaic (PV) solar energy to mitigate environmental concerns and reduce fossil fuel

dependency is evident worldwide, particularly in the Middle East. PV energy competes favorably with conventional power sources [4], prompting public administrations to promote PV installations in urban areas. The share of renewable energy in a nation's gross final energy consumption (TFEC) varies based on the energy mix. In 2021, many countries witnessed an increasing trend in renewable energy adoption. European countries demonstrated notable growth rates in their renewable energy shares. Asia, the USA, and Africa also experienced significant growth, as depicted in Fig. 1 [4].

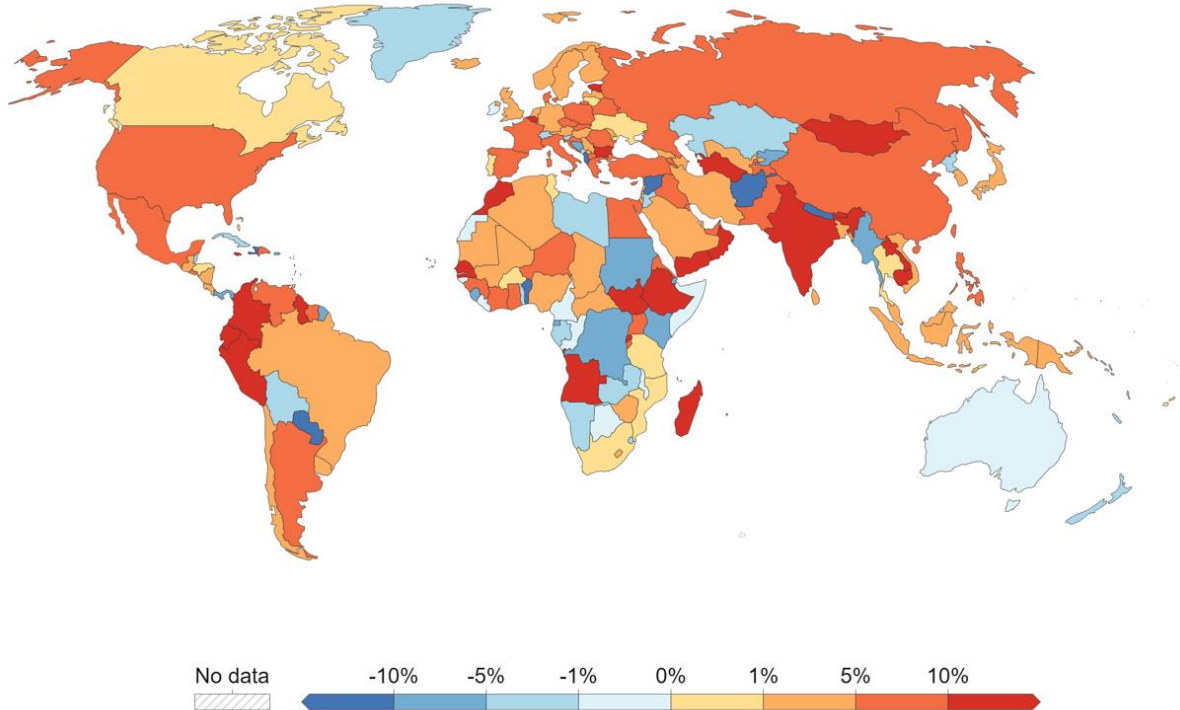


**Fig. 1** Renewable Energy Share in the World [4].

Integrating PV systems in urban areas is vital for energy conversion and is supported by global regulations and public policies. These policies include incentives like subsidies, soft loans, and tax reductions, besides simplified administrative procedures for installation and grid connection [5, 6]. Public power purchase agreements promote PV project deployment, and mechanisms like feed-in tariffs, feed-in premiums, and tradable green certifications incentivize renewable energy generation. Net metering and billing frameworks enable PV system owners to offset consumption with generated electricity. Research and development subsidies and demonstration programs advance PV technology and its urban integration [7]. One innovative approach to PV system implementation in urban planning is the Smartflower system. It is a compact, sun-tracking solar cell array with a unique design resembling a sunflower petal [8, 9]. PV cells exhibit nonlinear characteristics in their current-voltage (I-V) and power-voltage (P-V) curves, influenced by factors like solar radiation and temperature. Silicon-based PV cells, commonly used, have lower energy conversion efficiency, driving extensive research into improving efficiency. Effective cell modeling, including the popular single-diode model, aids in understanding PV system behavior and efficiency [10-12]. Saleh et al. [13] conducted a comprehensive review of PV systems, highlighting their pivotal role in energy production. They presented the paramount significance of energy generation. The study investigated different cooling techniques such as water-cooled and air-cooled. However, this study established the important function that PV solar systems play in enhancing energy generation efficiency. Jadallah et al. [14] examined a glass-to-glass PV module design to counter traditional module issues: yellowing and moisture. This strategy ensured that moisture did not accumulate and facilitated heat retention. Simulations and data sheet validations gave an output of 94.2W peak power with about 11.1% efficiency. Moisture permeation and yellowing is covered in this design, making it more durable with improved performance. The study contributes to knowledge about new technologies regarding efficiency and reliability of PV systems. Abdulmunem et al. [15] explored how filter colors impact the PV panel performance in Baghdad's unique weather conditions. Seven colored filters were assessed for their effect on electrical productivity and temperature changes using photonic theory and energy analysis. The study aimed to enhance the PV module efficiency in high-temperature climates. The results showed that the colored filters significantly influenced the PV technology. Red had the highest temperature,

while violet had the lowest, directly impacting electrical performance. Filters that reduced temperatures enhanced PV module efficiency remarkably. Mohammed and Mohammed [16] focused on optimizing solar panel energy capture. The study utilized solar tracker rotation for precise sun alignment. Astronomical calculations determine the sun's position according to latitude and longitude. The panels were horizontally oriented, adjusting through nine positions daily. Outcomes revealed a 17.3% rise in the daily power output with horizontal solar tracking compared to fixed panels. However, shading during sunrise and sunset caused a 2 to 3.5-hour energy loss. The shading dynamics varied with seasonal shifts and sun angles. Omer et al. [17] investigated diverse PV panel connections, including series, parallel, and combined setups (3p1s, 2p2s, and 2s2s). The goal was to identify the ideal connection for varying load speeds. Experimental data evaluated exergy efficiency, with 2p2p parallel connection emerging as the best at 43.77% efficiency. This research highlighted the pivotal role of connection configurations in optimizing the PV system performance, providing valuable insights for tailored designs and efficient system optimization. Al-shammari et al. [18] assessed a standalone PV system in Baghdad, optimizing panel sizing, energy demand, battery, inverters, and connections. Computational modeling compared design costs to conventional sources, revealing PV's potential as a self-sufficient alternative in areas with limited grid access. This research offered essential insights for decision-making in Baghdad and similar. Chaichan et al. [19] examined the influence of dust and pollution on PV solar cells in four Iraqi regions. Dust analysis unveiled mineral, pollutant, and particulate matter content. The experimental data indicated substantial voltage, current, and power output declines, emphasizing the necessity for maintenance strategies to ensure efficient PV solar system operation in these areas. Jamhour et al. [20] conducted PV module performance in Baghdad's climate. The study combined theoretical analysis and experiments. MATLAB analyzed open-circuit voltage, short-circuit current, output power, and efficiency. The numerical results were compared to experimental data, showing strong agreement. This research highlighted the PV module behavior in Baghdad's weather, validating theoretical accuracy through experimentation. Gaeid et al. [21] aimed to boost PV panel efficiency via energy optimization and temperature reduction using an Arduino Uno R3, relay kit, LDR, LM35 temperature sensor, high-efficiency solar panel, and satellite motor. Arduino Uno and Protuse software enabled precise control. Testing validated the satellite

motor's superior performance, reducing power consumption and improving efficiency. This cost-effective, automated approach effectively validated the tracking system's capabilities. Chaichan and Kazem [22] examined how dust affects energy production in Baghdad. These investigations involved studying of dust samples for two months with particulate matters, calcium carbonate, and soil effects. This proved that dust accumulation led to notable PV performance diminution. Energy loss due to dust composition led to declining in energy production and additional rise in elevated temperature of the panel. In this context, proper regular cleaning and maintenance were crucial to deter dust accumulation that reduced ideal PV system energy generation efficacy. Mohammed [23] proposed a new solar cell positioning algorithm looking toward two aims, such as maximization of the daylight capture, and tracking of optical communication signals in the nighttime. Transitioning easily from one mode of operation to another is inherent in a system with automated control. The algorithm's accuracy and precise positioning were tested in implementation and outdoor tests. It functioned with accuracy in detecting operational scenarios and showed perfect results. By measuring power generation and consumption, it was proven feasible by design, thus confirming its effectiveness. Mulyana et al. [24] utilized the SolidWorks program, designed, and simulations were done on a solar smart flower. Aspects that affected design included the various materials, interaction of components, and applied forces. This was done by means of static simulations that have shown a high degree of satisfaction on our part, thus allowing us to consider the further continuation onto the next stage – production. In a similar vein. Vedat [25] explored the impact of building orientation and slope on photovoltaic performance within urban settings. They proposed an analysis considering photovoltaic tracking systems to address residential site performance losses and aesthetic concerns. The study presented a solution through research and design analysis, ensuring that the system's roof dimensions align with the yearly energy demands of a household, which was achieved by employing simulation tools such as the "PV performance tool" to assess the annual energy production from photovoltaic panels. Kumar et al. [26] presented a solar tree design for the Himalayan region, creatively addressing land scarcity. The non-tracking modular tree integrated various devices' LED lights, USB ports, and sockets. It outperformed land-based systems by generating 28% more power, yielding 2160 to 2520 units annually. With a safety factor of 6 at 100 km/h wind speed, it also

improved energy density (42.37%) and solar footprint (39.47%) compared to land-based setups during sunny conditions. Collectively, these studies demonstrate continuous exploration and innovation in solar energy applications. They span from integrating solar tech into aesthetic designs to optimizing residential photovoltaic systems. These studies contribute to advancing sustainable energy solutions and improving solar energy efficiency by investigating panel design, orientation, and performance intricacies. The Smartflower system revolutionizes PV energy deployment. Inspired by sunflowers, it seamlessly blends energy generation with aesthetics, surpassing traditional PV setups. It employs articulated solar cells with dynamic tracking, boosting efficiency through optimized solar exposure. Beyond energy generation, it impacts urban planning, aesthetics, and public engagement with renewables [27]. The study investigates renewable energy potential, urban dynamics, and technological advancement. Investigating the Smartflower system's impact highlights its potential to reshape urban energy dynamics and the evolving energy landscape. While prior research explores PV integration in urban contexts, a gap remains in evaluating system performance in real-world settings, including electrical, mechanical, and safety challenges. This study analyzes solar panel performance for Smartflower integration by optimizing efficiency and behavior under varying conditions. The methodology involves real-scenario data collection, I-V and P-V curves for insights, and exploring solar radiation and temperature impacts. Validation ensures accurate outcomes of a Smartflower panel proposed for urban.

## 2. MATHEMATICAL MODELING

The studied single-diode model is shown in Fig.2, which also shows the P-V and I-V characteristics curves of an exemplary PV module [28]. The equation demonstrating this model is transcendental, and its nature is implicit, so its solution must involve significant computational complications and might require many approximations and simplifications [29]. The main issue of modeling a PV system is represented by the most known fact that the characteristic curves of any PV module are highly dependent on temperature and insolation, which vary continuously in nature [30]. A PV module datasheet usually only provides the module's parameters under standard conditions (STC). Accordingly, the included parameters sufficient to model a PV module are extracted at STC; this extracted information should be correlated according to the predominant irradiance and temperature [31].

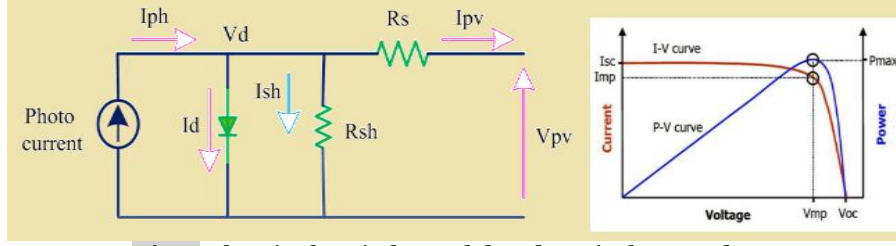


**Fig.2** The Single-Diode Model and Typical I-V and PV Characteristics of a PV Module.

The single-diode model shown in Fig. 2 is widely adopted for modeling a PV module due to its simplicity. The terminal voltage  $V$  and current  $I$  are associated by the below implicit transcendent equation [32]:

$$I = I_{ph} - I_{sat} \left[ \exp\left(\frac{V+IR_s}{n N_s V_{th}}\right) \right] - \frac{V+IR_s}{R_{sh}} \quad (1)$$

where  $V_{th} = \frac{kT}{q} = 25.7 \text{ mV at } 25 \text{ C}$ .

The five unknown common parameters that must be determined are photocurrent source  $I_{ph}$ , saturation current  $I_{sat}$ , ideality factor  $n$ , series  $R_s$ , and shunt  $R_{sh}$  resistances of the module. The manufacturer's datasheet usually includes data at the prominent points, i.e., short-circuit current  $I_{SC}$ , open-circuit voltage  $V_{OC}$ , maximum power point MPP, current  $I_m$ , and voltage  $V_m$ . The short-circuit current  $I_{SC}$  and open-circuit voltage  $V_{OC}$  temperature coefficients may be listed. Therefore, five equations must be solved to determine the five parameters of any PV module. The amazing points can be utilized to obtain the following three equations [33]:

$$OS: (V_{OC}, 0): 0 = I_{ph} - I_{sat} \left[ \exp\left(\frac{V_{OC}}{n N_s V_{th}}\right) - 1 \right] - \frac{V_{OC}}{R_{sh}} \quad (2)$$

$$SCP (0, I_{SC}): I_{SC} = I_{ph} - I_{sat} \left[ \exp\left(\frac{I_{SC} R_s}{n N_s V_{th}}\right) - 1 \right] - \frac{I_{SC} R_s}{R_{sh}} \quad (3)$$

$$MPP: I_m = I_{ph} - I_{sat} \left[ \exp\left(\frac{V_m + I_m R_s}{n N_s V_T}\right) \right] - \frac{V_m + I_m R_s}{R_{sh}} \quad (4)$$

In addition, the derivative  $dP/dV = 0$  at the MPP is used to develop Eq. (5):

$$\frac{dP}{dV} \Big|_{MPP} = -\frac{I_m}{V_m} = \frac{\frac{1}{R_{sh}} \frac{I_{sat}}{n N_s V_{th}} \exp\left(\frac{V_m + I_m R_s}{n N_s V_T}\right)}{1 + \frac{R_s}{R_{sh}} + \frac{I_{sat} R_s}{n N_s V_{th}} \exp\left(\frac{V_m + I_m R_s}{n N_s V_T}\right)} \quad (5)$$

Ultimately, the reciprocal of the I-V curve slope at the short circuit point utilized to generate Eq.(6) necessary for parameter determination of the model:

$$\frac{dP}{dV} \Big|_{I_{SC}} = -\frac{1}{R_{sho}} = \frac{\frac{1}{R_{sh}} \frac{I_{sat}}{n N_s V_T} \exp\left(\frac{I_{SC} R_s}{n N_s V_T}\right)}{1 + \frac{R_s}{R_{sh}} + \frac{I_{sat} R_s}{n N_s V_T} \exp\left(\frac{V_m + I_m R_s}{n N_s V_T}\right)} = -\frac{1}{R_{sh}} \quad (6)$$

Equations from Eq. (2) to Eq. (6) can be solved numerically using Newton-Raphson or iterative methods. Furthermore, many approaches evaluate the single diode model's five parameters, which also need the manufacturer's datasheet information and iterative processes [34]. Furthermore, this paper focuses only on the temperature and irradiance variations and introduces a review of common methods to deal with these variations of each parameter, as presented below:

### 2.1.Short-Circuit Current

The short circuit current  $I_{SC}$  can be expressed by two methods depending on irradiance ( $G$ ) and temperature ( $T$ ) by using the linear empirical equation [35]:

$$I_{sc}(G, T) = \frac{G}{G_{STC}} [I_{sc,STC} + \mu_{I_{sc}}(T - T_{sc})] \quad (7)$$

Eq. (7) leads to a deviation between the short circuit current value and the experimental results due to the solar irradiance nonlinearity. This nonlinearity can be correlated by introducing the exponent  $\alpha$  [35] as:

$$I_{sc}(G, T) = \left(\frac{G}{G_{STC}}\right)^\alpha [I_{sc,STC} + \mu_{I_{sc}}(T - T_{sc})], \text{ where } \alpha = \frac{\ln\left(\frac{I_{sc,STC}}{I_{sc}}\right)}{\ln\left(\frac{G_{STC}}{G}\right)} \quad (8)$$

### 2.2.Open-Circuit Voltage

The effect of  $G$  and  $T$  on  $V_{oc}$  can be expressed by many methods, as explained below:

The simplest of these methods neglects the insolation effect [36], so:

$$V_{oc}(T) = V_{oc,STC} + \mu_{V_{oc}}(T - T_{STC}) \quad (9)$$

while the  $V_{oc}$  dependency on the insolation could be derived using Eq. (2), resulting in:

$$V_{oc}(G) = \ln\left(\frac{I_{ph}(G) R_{sh} - V_{oc}(G)}{I_{sat} R_{sh}}\right) n N_s V_{th} \quad (10)$$

Eq. (10) can be numerically solved by using the Newton-Raphson method. The  $V_{oc}$  dependency on the temperature can be achieved using Eq.(9) [35]. Also, the  $V_{oc}$  dependency on temperature and insolation can be obtained from Eq. (2) [34], yielding:

$$V_{oc}(G, T) = V_{oc,STC} + \frac{N_s k T}{q} \ln(G) + \mu_{V_{oc}}(T - T_{STC}) \quad (11)$$

Also, a derivative of an interpolation relationship between  $V_{oc}$  through  $G$  and  $T$  gives:

$$V_{oc}(G, T) = V_{oc,STC} + C_1 \ln\left(\frac{G}{G_{STC}}\right) + C_2 \ln\left(\frac{G}{G_{STC}}\right)^2 + C_3 \ln\left(\frac{G}{G_{STC}}\right)^3 + \mu_{V_{oc}}(T - T_{STC}) \quad (12)$$

where  $C_1 = 5.4685 \times 10^{-2}$ ,  $C_2 = 5.97387 \times 10^{-3}$ , and  $C_3 = 7.61618 \times 10^{-4}$  for silicon. Moreover, the three equations below describe the nonlinearity of  $G$  and  $T$  on  $V_{oc}$  [32, 35, 36]:

$$V_{oc}(G, T) = \frac{V_{oc,STC}}{1 + \beta \left(\frac{G_{STC}}{G}\right)} \left(\frac{T_{STC}}{T}\right)^\gamma \quad (13)$$

$$\text{where } \beta = \frac{\left(\frac{V_{oc,STC}}{V_{oc,G}}\right)^{-1}}{\ln\left(\frac{G_{STC}}{G}\right)}, \gamma = \frac{\ln\left(\frac{V_{oc,STC}}{V_{oc,T}}\right)}{\ln\left(\frac{T}{T_{STC}}\right)}$$

### 2.3. Photocurrent Current

Photocurrent  $I_{ph}$  can be presented utilizing various model specifications with the datasheet given information. Thus, several representations for evaluating this current are stated below. The saturation current  $I_{sat}$  and series resistance  $R_s$  can be ignored in Eq. (3); consequently,  $I_{ph} = I$ . While, when the effect of the resistances is considered in Eq. (3), the photocurrent becomes [35]:

$$I_{ph} = \frac{R_{sh} + R_s}{I_{sc} * R_{sh}} \quad (14)$$

Moreover, using Eq. (2) and Eq. (3), the photocurrent can be written as:

$$I_{ph} = I_{sat} \exp\left(\frac{V_{oc}}{n N_s V_{th}}\right) + \frac{V_{oc}}{R_{sh}} \quad (15)$$

which, according to the assumption of  $V_{oc}$  and  $I_{sat}$ , depends only on the temperature. So,

$$I_{ph}(T) = \frac{I_{sat}(T) \exp\left(\frac{V_{oc,STC} + \mu_{V_{oc}}(T - T_{STC})}{n N_s V_{th}}\right) + \frac{V_{oc,STC} + \mu_{V_{oc}}(T - T_{STC})}{R_{sh}}}{R_{sh}} \quad (16)$$

If Eq. (2) and Eq. (3) are combined without ignoring any terms, the magnitude of the photocurrent is:

$$I_{ph,STC} = \left(1 + \frac{R_s}{R_{sh}}\right) I_{sc,STC} \exp\left(\frac{V_{oc,STC}}{n N_s V_{th}} - 1\right) + \frac{\frac{V_{oc,STC}}{R_{sh}} \left[1 - \exp\left(\frac{I_{sc,STC} R_s}{n N_s V_{th}}\right)\right]}{\exp\left(\frac{V_{oc}}{n N_s V_{th}}\right) - \exp\left(\frac{I_{sc,STC} R_s}{n N_s V_{th}}\right)} \quad (17)$$

### 2.4. Dark Saturation Current

Previous works generally suggested a very high dependence of the saturation current  $I_{sat}$  on the temperature, while others showed that the

saturation current can also be increased with insolation [33]. However, the important effect of this current on the I-V curve can be described in five general methods, as shown below [37]. From Eq. (2) and Eq. (3) with datasheet information, saturation current variations with temperature could be obtained as [37].

$$I_{sat}(T) = I_{sc,STC} + \mu_{I_{sc}}(T - T_{STC}) - \frac{V_{oc,STC} + \mu_{V_{oc}}(T - T_{STC}) - (I_{sc,STC} + \mu_{I_{sc}}(T - T_{STC})) R_s}{\exp\left(\frac{V_{oc,STC} + \mu_{V_{oc}}(T - T_{STC})}{n N_s V_{th}(T)}\right) * R_{sh}} \quad (18)$$

Considering that the saturation current is considering the semiconductor bandgap and the temperature [32,35,37], also, using Eq. (2) and Eq. (3), the saturation current may be written as [37], and if  $R_{sh} = \infty$ ,  $I_{sc,STC} = I_{ph}$ , and  $I_{sat}$  is achieved from open circuit voltage at STC [35]:

$$I_{sat}(G, T) = \frac{\left(\frac{G}{G_{STC}}\right) \left(I_{sc,STC} + \mu_{I_{sc}}(T - T_{STC})\right) \exp\left(\frac{q \mu_{V_{oc}}(T - T_{STC})}{n N_s k V_T}\right)}{\left(\frac{I_{sc,STC}}{I_{sc,STC} + 1}\right)^{\frac{T_{STC}}{T}} - \exp\left(\frac{q \mu_{V_{oc}}(T - T_{STC})}{n N_s k V_T}\right)} \quad (19)$$

### 2.5. Series and Shunt Resistances

The effect of temperature and irradiance variations on the resistances can be described as follows. The temperature and irradiance effect on the resistances is neglected [38], i.e.,  $R_s(G, T) = R_{s,STC}$ , and  $R_{sh}(G, T) = R_{sh,STC}$ . Also, the series resistance is assumed to be constant, i.e.,  $R_s(G, T) = R_{s,STC}$ . While the shunt resistance varies with the solar irradiance as [33, 35, 38].

$$R_{sh}(G, T) = \left(\frac{G_{STC}}{G}\right) R_{sh,STC} \quad (20)$$

The series resistance decreases with insolation and increases with temperature; the shunt resistance varies with the insolation, as in Eq.(20), so the series resistance is [34].

$$R_s(G, T) = \left(\frac{T}{T_{STC}}\right) \left(1 - \lambda \ln \frac{G}{G_{STC}}\right) R_{s,STC} \quad (21)$$

where  $\lambda = 0.217$

## 3. DESIGN AND FEATURES OF SMARTFLOWER

The Smartflower system, highlighted in Fig. 3, was designed precisely using SOLIDWORKS software and incorporates key elements like the photovoltaic panel petal, dual-axis rotation mechanism, and base. This innovative design enables remarkable functionality, with automated petal movements spanning 360 degrees to dynamically align with the sun's path for maximum solar energy capture. The system's vertical mobility adapts to varying sunlight angles, optimizing energy production. Visually, the Smartflower system stands out, employing color matching and advanced manufacturing techniques to blend aesthetics with function, distinguishing it from conventional photovoltaic installations. This

design integrates renewable energy seamlessly into public spaces. The system excels with its compact tree-like structure, ideal for urban settings, efficiently utilizing limited space. It generates power and provides shaded areas beneath its circular solar leaves for public use. Additionally, the main rod serves as storage and battery housing, simplifying installation and enhancing efficiency. In summary, the Smartflower system represents a significant advancement in solar technology, offering an innovative design and functionality for efficient, visually appealing renewable energy generation. Its integration into public spaces and optimal land use make it a compelling solution for urban solar power adoption.

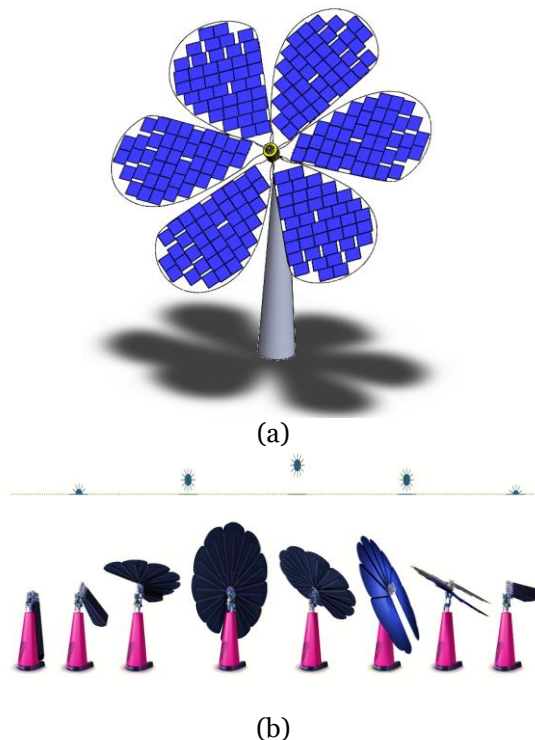


**Fig. 3** (a) The Smart Sunflower Designed in SOLIDWORKS. (b) The Smart Sunflower and its Sequence of Opening and Settling [39].

#### 4. EXPERIMENTAL SETTING

Utilizing locally available materials was pivotal in ensuring the cost-effectiveness and simplicity of the solar panel construction. Forty-two solar cells measuring  $13 \times 14$  cm were affixed to a 0.5 mm aluminum layer. The manufacturing process of the PV Smartflower panel, as depicted in Fig. 4, entails several distinct stages:

- **Stage 1:** The initial step involves printing the PV Smartflower panel's design on paper, preserving its precise dimensions and size, and serving as a blueprint for subsequent manufacturing.
- **Stage 2:** Advancing the creation of an iron frame that replicates the exact shape of the PV panel, providing a standardized

platform for uniform manufacturing and ensuring consistent dimensions.

- **Stage 3:** Focusing on refining the iron platform according to the requirements for assembling the PV panels.
- **Stage 4:** Preparation of the small solar cells to optimize their integration with the proposed PV panel.
- **Stage 5:** Meticulous installation of prepared PV cells onto an aluminum sheet, affixed on the aluminum frame in a pattern mimicking sunflower petals, forming the fundamental PV panel structure.
- **Stage 6:** The final stage involves connecting the PV cells in parallel and series configurations to achieve the desired voltage and current levels, ultimately delivering the intended power output.

This detailed manufacturing process ensures uniformity, efficiency, and precision in PV Smartflower panel assembly, resulting in panels with a distinct sunflower petal shape optimized for electrical power output. Performance data collection occurred in Baghdad, Iraq, on a residential building's rooftop (approximately  $44^\circ 25' 16''$  E longitude and  $33^\circ 19' 34''$  N latitude). Various electric, atmospheric, and irradiance measuring devices captured data under irradiance levels ranging from  $150\text{-}1000$   $\text{W}/\text{m}^2$ . The PV module underwent calibration according to standard testing conditions. The electrical interconnection of the constituent cells within the solar panel is presented in Fig. 5 for a visual representation. The SolidWorks model assigns each cell a numerical identifier and specific location within the panel structure. Notably, six adjacent cells have been systematically arranged in a series configuration to generate the requisite voltage, approximately  $V_{oc}=64.8$  V. Subsequently, these series-connected sets were organized into seven parallel rows. These connections culminated in the designed panel possessing a net capacity of 84 W. A sophisticated Solar Panel multimeter, as depicted in Fig. 6 with an LCD screen, precisely recorded key parameters, such as maximum solar power, voltage, and current. These data generated characteristic curves, offering comprehensive insights into the module's performance. The depicted test system consisted of a thermocouple for temperature measurement, a voltmeter for voltage measurement, and an ammeter for current measurement Fig. 7 A typical curve was constructed for determining parameters like maximum power point, short circuit current, and open circuit voltage. A specialized solar meter measured normal irradiance (G), while an equivalent cell temperature (ECT) was derived from the open circuit voltage measurements.

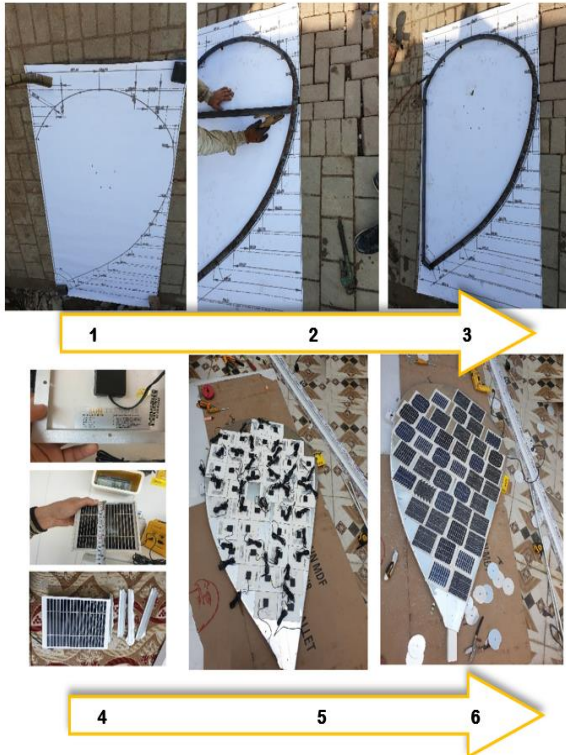


**Fig. 4** The Manufacturing Stages of the Sunflower Solar Panel.

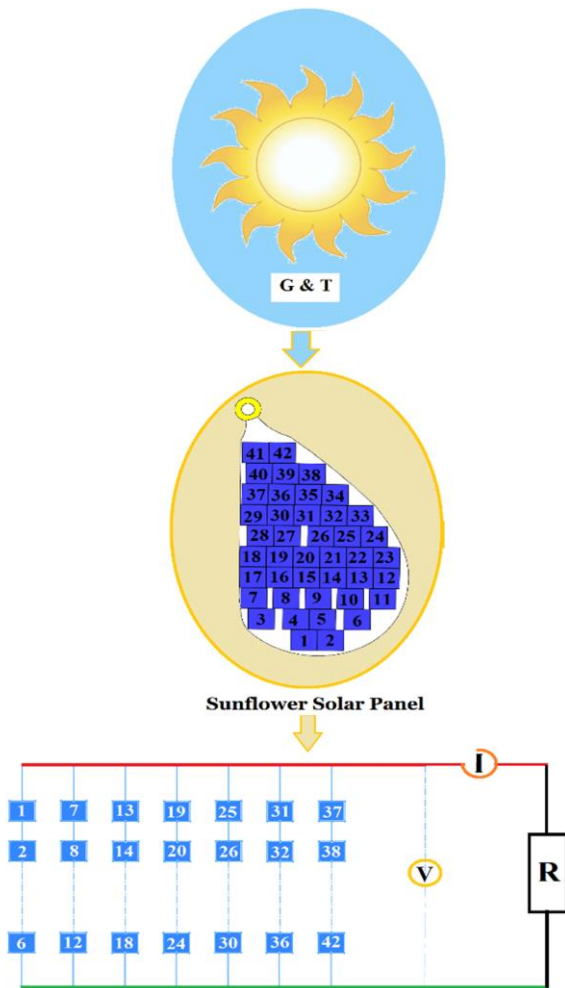


**Fig. 5** The Electric Circuit Configuration.



**Fig. 6** LCD Photovoltaic Solar Panel Multimeter MPPT Tester.

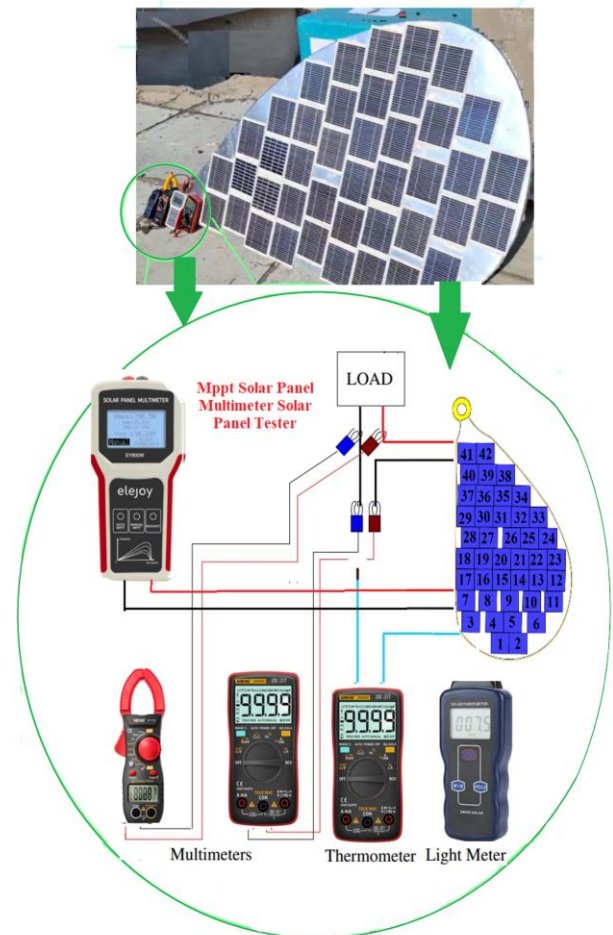


**Fig. 7** Schematic Diagram of the Experimental Setting.

### 5.RESULTS AND DISCUSSION

The present study rigorously assessed a proposed solar panel, conducting precise experiments to collect voltage, current, and power data. The data collection process was meticulously planned and executed using specialized instruments. The experimental setup simulated real-world scenarios, controlling parameters such as irradiance and temperature. Advanced sensors and data



systems yielded precise measurements. The data formed the basis for critical I-V and P-V curves, revealing key performance metrics. To validate the proposed model, the outdoor measurements of a single petal module were rigorously compared to the simulation results. This evaluation aimed to confirm the model's ability to capture the panel's behavior under diverse conditions. Standard conditions, i.e., 1000 W/m<sup>2</sup> irradiance and 25°C module temperature, were selected for experimental relevance and practical applicability. As shown in Fig. 8., there are analytical steps involved in determining the calculated parameters from input variables. This is followed by experimental testing whereby it is compared with the results obtained analogously. This is a sequential chain of events used in the study leading to its analytical and experimental findings as shown below. Sophisticated statistical analysis tools were applied in the comparison between experimentally obtained values, and the obtained simulation results. A complete analysis was undertaken to assess the correctness and authenticity with which this theory explained the dynamics of the solar panel process. Data acquired experimentally and simulation resulted in characteristic curves for picked modules. These curves provide a visual representation of how the panel performs at various current, voltage, and power levels, which is important information when it comes to understanding the panel's operation under differing circumstances. These curves were minutely analyzed so as to make future predictions and optimizations with regard to power generation and system efficiency. According to Fig. 9, the expected output power was 84W. This result proved the appropriateness as well as effectiveness of the suggested analytical model at the same time serving as a reference point for assessing the practicality of the panel efficiency determination. The I-V and P-V characteristic curves of the solar modules as operated during different solar irradiation level from 0.15 kW/m<sup>2</sup> up to 1kW/m<sup>2</sup> are presented next. This in-depth analysis explained how solar radiation change affected the panel's output. The solar radiation-power relationship is clearly depicted by the plotted curves of Fig. 10 and Fig.11 where enhanced solar radiation results in more power production. Insolation is referred to as intensity of solar radiation and affected directly the power output of PV system. This positive correlation can be attributed to the fundamental theory of PV panel operation and the photovoltaic effect. Photovoltaic effect involves excited electrons in a semiconductor material under direct exposure to the light photons from the sun, which gives rise to an electrical charge. Due to such, the amount of photons that come into contact with the face of

the PV panels is influenced by how intense the solar ray is.

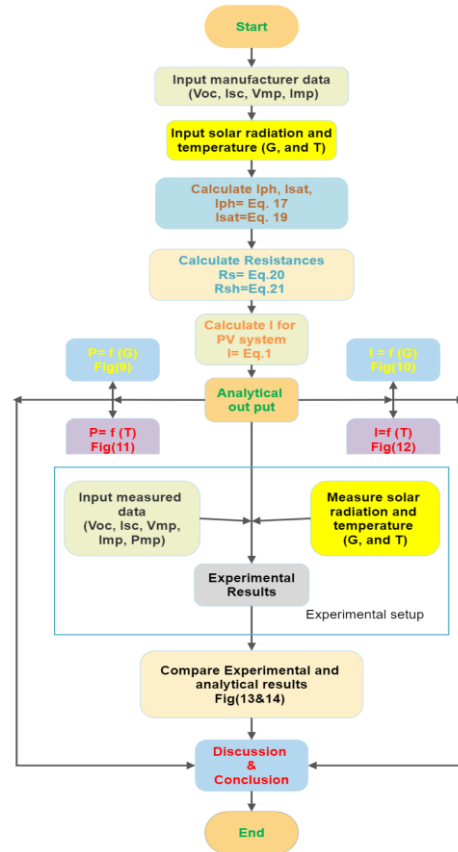


**Fig.8** Flowchart Depicting Analytical and Experimental Processes in the Study.

Increasing solar radiation means that there will be many photons available to interact with the semiconductor material thus electron excitation rate increases leading to increased electric current generation. In practical sense, this correlation has important consequences in respect of design and operation of the PV systems. This emphasizes the need for PV panel placement in well-lit areas so as to increase the electrical energy generated. In addition to this, the importance of such monitoring system becomes apparent as it should be designed in a way to automatically turn the panels to face directly towards the moving sun during a whole day. Moreover, the positive relationship between solar radiation and power output strengthens the notion that solar is renewable and plentiful. However, it could be noted that PV installations are best suited for regions with high solar radiation levels since such places demonstrate greater PV power generating capability. This correlation further drives research towards the development of more efficient PV technologies leveraging on different solar radiation strengths for increased energy yield and a sustainable energy prospect. Finally, the increasing trend between solar radiation and power output depicted in the graphs Fig. 10 and Fig. 11 is consistent with the photo-voltaic principle. The direct influence of

sunlight energy on the production of electrical current by PV panel as seen above, solar radiation is paramount element for optimal performance of photovoltaic systems. Also, the effect of temperature on the efficiency of the PV modules is analyzed, as presented in Fig. 12 and Fig. 13. Solar panels have power output which is highly dependent on the temperature variations. The collected experimental data allowed a detailed consideration of the behavior of the panel under different temperature conditions. Temperature is one of the most critical factors affecting the performance of PV panels whose behavior and efficiency depends much on it. Temperature affects a multiplicity of crucial variables cumulatively, determining a PV system's total yield and performance. With an increase in temperature, charge movements within the semiconductor material of a PV panel become more vigorous resulting in an increased short circuit current ( $I_{sc}$ ) defined as the maximum current produced by a PV panel that has been short-circuited. The response results from a large proportion of free moveable charges that are conducting this current. On the other hand, higher temperatures decrease the width of the semiconductor gap. The bandgap is defined as an energy gap between the valence band where the electrons are bounded and the conduction band in which the electrons are free moving. As a result, the bandgap was reduced which led to lower  $V_{oc}$ . This occurs due to a reduction in the amount of energy needed to move an electron from the valence band to the conduction band which results in a low voltage potential between the PV cells. In sum, temperature-induced changes in both  $I_{sc}$  and  $V_{oc}$  together affect the MPPT performance of a PV panel. The MPP is the operating position of the lowest possible current and the highest possible voltage where the panel generates the maximum power. Shifts in the MPP occur due to the interaction between temperature-induced alterations in  $I_{SC}$  and  $V_{oc}$ . Practically, this means increases in  $I_{SC}$  with high temperatures but reduction of  $V_{oc}$ , and with this, a reduced bandgap. Therefore, this

balance could affect the total power generation capacity. PV panel is also affected by temperature in terms of its resistance. As for resistance inside of the panel it raises with the increase in temperature. This phenomenon is attributed to factors such as high phonon scattering, greater lattice vibrations. Increase in resistance implies high energy losses and poor conversion efficiency. On the other hand, lower temperatures led to a decrease in resistance thereby increasing energy generation effectiveness. The comprehension of these multi-dimensional thermal phenomena is vital in achieving efficient solar PV setup, improving its efficiency, and forecasting its operation under different climactic settings. The fact that temperature's effect is contemporaneous shows how difficult it may be to obtain maximum energy production and efficiency from a PV panel. A comprehensive comparison was performed between the measurement curves for the sunflower PV module and the corresponding analytical curves with an aim at validating the accuracy and reliability of the modeling approach as well as the experimental methods used. The process of this thorough validation entailed examination of several statistically-derived measures drawn out of different data sets. The relative comparison is presented at Fig. 14 and Fig. 15, showing how accurately they match the current analytical method. The uniformity was impressive, which constituted very reliable proof that the modeling performed properly as well as the measurement itself was exact. The current research reveals detailed information on the solar panels' performance of the suggested Smartflower system. Accuracy is ensured through rigorous data collection, analysis, and validation. This analytical model reveals how a panel changes its behaviour in different conditions stressing the impact of solar radiation and ambient temperature towards optimization. This has aided in improving solar technology, hence enhancing on efficiency and sustainability.

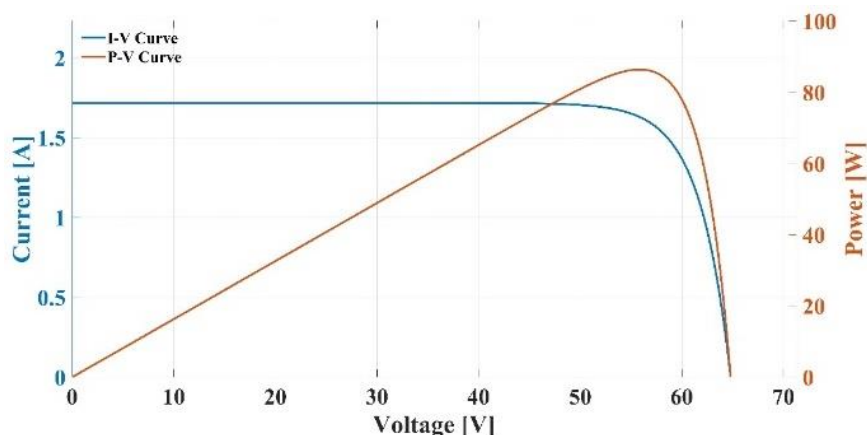
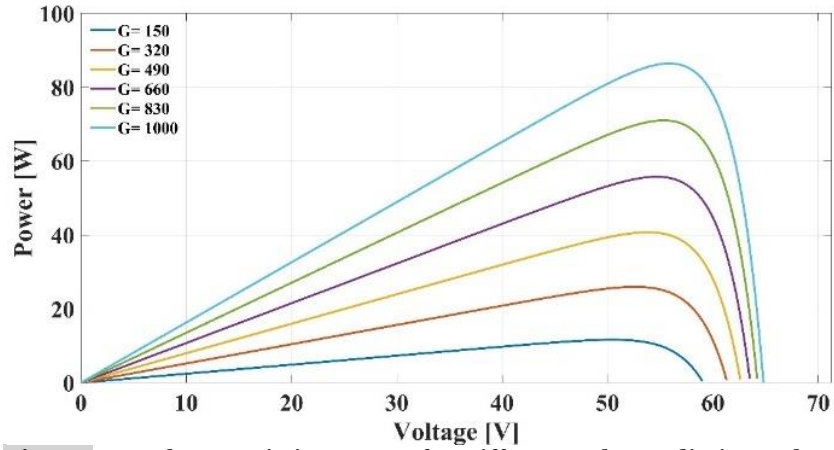
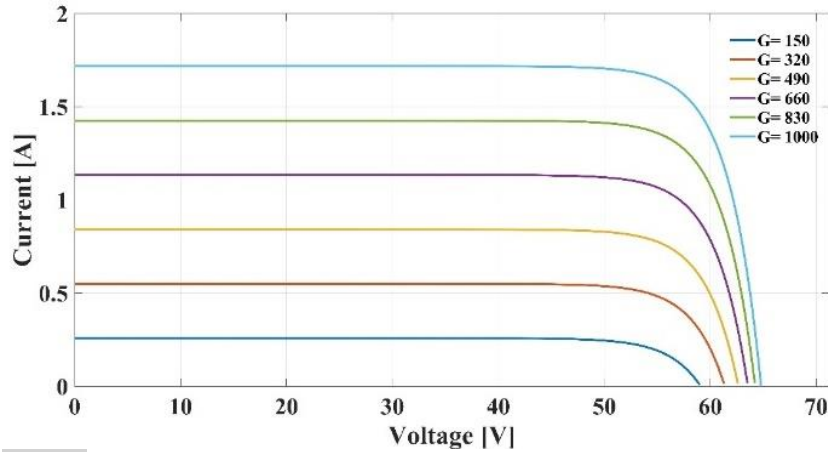


Fig. 9 PV Panel Characteristics Curves.



**Fig. 10** P-V Characteristics Curves for Different Solar Radiation Values.



**Fig. 11** I-V Characteristics Curves for Different Solar Radiation Values.

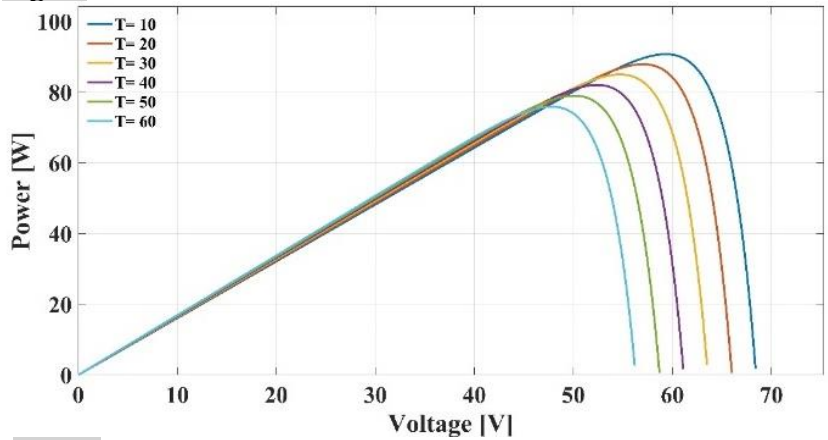


**Fig. 12** P-V Characteristics Curves for Different Temperature Values.

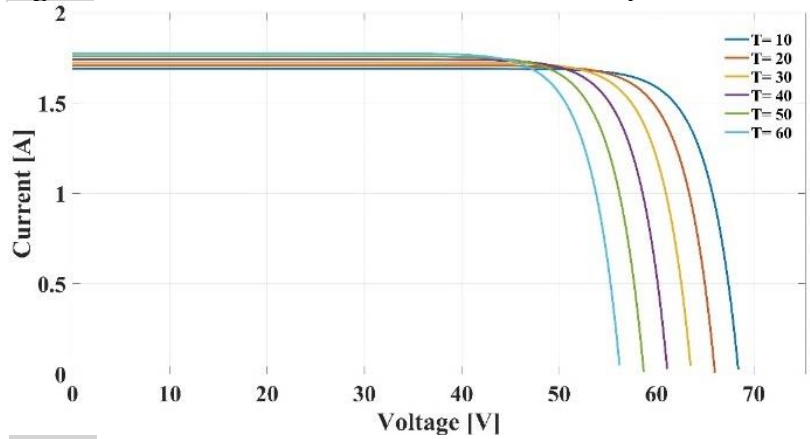


**Fig. 13** I-V Characteristics Curves for Different Temperature Values.

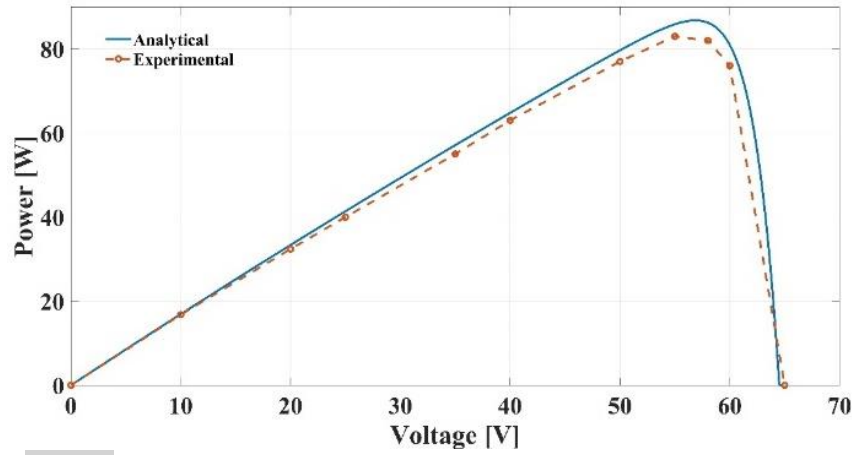


**Fig. 14** P-V Characteristics Curve with Experimental Measured Data.

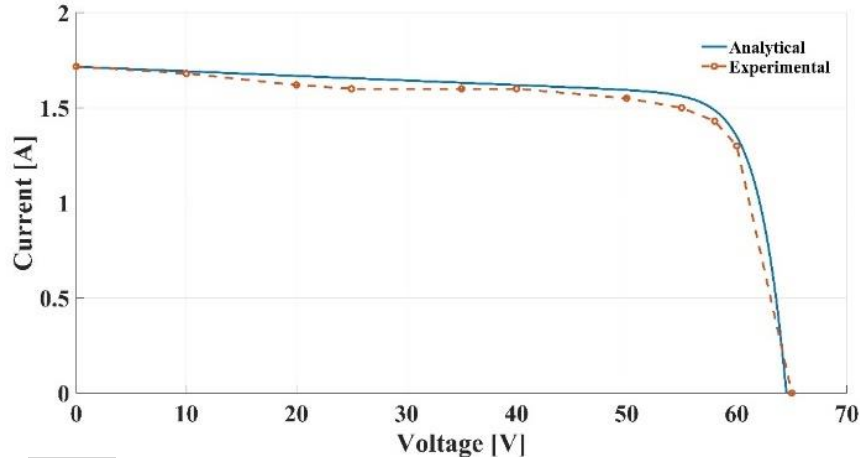


**Fig. 15** I-V Characteristics Curve with Experimental Measured Data.

## 6. CONCLUSION

The present investigation introduces an innovative approach involving designing, producing, and evaluating a specialized photovoltaic (PV) panel for integration into the Smartflower system. The focus is on analyzing the panel's performance under various operational conditions. The Smartflower system, inspired by sunflowers, offers a unique energy generation solution, incorporating flexible solar cells for efficient sun-tracking. A key finding is the direct correlation between high solar radiation and improved PV panel efficiency. Increased radiation significantly increased the power output; a 104% radiation increase resulted in a remarkable 115% peak power production boost and a parallel 100% output current enhancement. Conversely, high temperatures reduced the power output, with a 400% temperature increase reducing the power generation by 11.1%. The alignment of empirical observations and analytical outcomes validated the proposed model's accuracy, reinforcing result reliability. This research advances the Smartflower system's manufacturing process, including control mechanisms, tracking capabilities, and the energy-generation framework, paving the way for optimized energy utilization and promising integration into real-world applications.

## NOMENCLATURE

$G$	Solar irradiance ( $W/m^2$ )
$G_{stc}$	Solar irradiance at standard rating conditions ( $1000 W/m^2$ )
$I$	Current generated by panel (A)
$I_d$	Diode current (A)
$I_{ph}$	Photocurrent (A)
$I_{mp}$	Current at the maximum power point (A)
$I_{sc}$	Panel short circuit current (A)
$I_{sat}$	Saturation current (A)
$K$	Thermal correction factor ( $\Omega/^\circ C$ )
$k$	Boltzmann constant ( $(1.381 \times 10^{-23}) J/K$ )
$n$	Diode quality factor
$P$	Power generated by the PV panel (W)
$q$	Electron charge ( $1.602 \times 10^{-19} \text{ } ^\circ C$ )
$R_L$	Electrical load ( $\Omega$ )
$R_s$	Series resistance ( $\Omega$ )
$R_{sh}$	Shunt resistance ( $\Omega$ )
$V$	Voltage generated by the PV panel (V)
$V_{mp}$	The maximum power point voltage (V)
$V_{oc}$	Open circuit voltage of the panel (V)
$\mu I_{sc}$	Short circuit current Thermal coefficient ( $A/\text{degc}$ )
$\mu V_{oc}$	Thermal coefficient of the open circuit voltage ( $V/\text{degc}$ )

## REFERENCES

- [1] Aslam A, Khan AN, Ahmed N, Ahmed N, Imran K, Mahmood M. **Effect of Fixed and Seasonal Tilt Angles on the Performance of an ON-Grid PV Plant.** *International Conference on Emerging Power Technologies (ICEPT) 2021*; Topi, Pakistan. IEEE: p. 1-5
- [2] Sengupta M, Habte A, Wilbert S, Gueymard C, Remund J. **Best Practices Handbook for the Collection and Use of Solar Resource Data for Solar Energy Applications.** Third Edition. Golden, CO: National Renewable Energy Laboratory; 2021.
- [3] Aslam A, Ahmed N, Qureshi SA, Assadi M, Ahmed N. **Advances in Solar PV Systems; A Comprehensive Review of PV Performance, Influencing Factors, and Mitigation Techniques.** *Energies* 2022; **15**(20): 7595, (1-52).
- [4] REN21. **Renewables 2022 Global Status. Global Status Report for Buildings and Construction: Towards a Zero-emission, Efficient and Resilient Buildings and Construction Sector.** 2022.
- [5] Agrawal R, Agrawal S, Samadhiya A, Kumar A, Luthra S, Jain V. **Adoption of Green Finance and Green Innovation for Achieving Circularity: An Exploratory Review and Future Directions.** *Geoscience Frontiers* 2023; 101669, (1-14).
- [6] Yu-Jui Chang I-YLH. **Transitioning From Illegal Rooftop Dwellings to Solar PV: Market-Based Incentive Design and Techno-Economic Analysis.** *Energy Strategy Reviews Contents* 2023; **49**: 101154, (1-9).
- [7] Vargas-Salgado C, Aparisi-Cerdá I, Alfonso-Solar D, Gómez-Navarro T. **Can Photovoltaic Systems be Profitable in Urban Areas? Analysis of Regulation Scenarios for Four Cases in Valencia City (Spain).** *Solar Energy* 2022; **23**: 461-477.
- [8] Van't Klooster T. **Kinegrity: Sun Directed Solar Cells.** Delft University of Technology, 2017.
- [9] The Environmental Center for ArabTowns. **Sustainable Ideas & Projects Shaping Future Cities.** *Envirocities eMagazine* 2017; **17**:1-44.
- [10] Babu PJS, Padmanabhan TS, Ahamed MI, Sivaranjani A. **Studies on Copper Indium Selenide/Zinc Sulphide Semiconductor Quantum Dots for Solar Cell Applications.** *Chalcogenide Letters* 2021; **18**(11):701-715.
- [11] Senthilkumar S, Mohan V, Mangaiyarkarasi SP, Karthikeyan M. **Analysis of Single-Diode PV Model and Optimized MPPT Model for Different Environmental Conditions.** *International Transactions on Electrical Energy Systems* 2022; **2022** :1-17.
- [12] Mathew LE, Panchal AK. **A Complete Numerical Investigation on Implicit and Explicit PV Single-Diode-Models Using I- and V-Approaches.** *IEEE Journal of Photovoltaics* 2021; **11**(3):827-837.
- [13] Saleh W, Jadallah A, Shuraiji A. **A-Review for the Cooling Techniques of PV/T Solar Air Collectors.** *Engineering and Technology Journal* 2022; **40**(1):129-136.
- [14] Jadallah AA, Hanfesh AO, Jebur TH. **Design, Fabrication, Testing and Simulation of a Modern Glass to Glass Photovoltaic Module in Iraq.** *Journal of Engineering Science and Technology* 2018; **13**(9):2750-2764.
- [15] Abdulmunem AR, Jadallah AA, Hoshi HA, Jabal MH. **Effect of Colored Filters on PV Panels Temperature and Performance under Baghdad Meteorological Condition.** *Tikrit Journal of Engineering Sciences* 2018; **25**(4):46-50.
- [16] Mohammed GA, Mohammed ZS. **Modeling Horizontal Single Axis Solar Tracker Upon Sun-Earth Geometric Relationships.** *Tikrit Journal of Engineering Sciences* 2022; **29**(3):43-48.
- [17] Omer D, Mahdi M, Shuraiji A. **Experimental Exergetic and Energetic Analysis of Different (PV) Array Configurations.** *Engineering and Technology Journal* 2022; **40**(1):82-89.
- [18] Al-shammara SA, Karamallah AA, Aljabair S. **Programing and Procedure Design of Stand-alone PV System for Clean Energy Home Supply in Baghdad.** *Engineering and Technology Journal* 2021; **39**(7): 1164-1173.
- [19] Chaichan MT, Kazem HA, Al-Waeli AHA, Sopian K. **The Effect of Dust Components and Contaminants on the Performance of Photovoltaic for the Four Regions in Iraq: A Practical Study.** *Renewable Energy and Environmental Sustainability* 2020; **5**(3):1-7.
- [20] Jamhour A, Numan AH, Hussein HA. **Theoretical and Experimental Performance Investigation of a Photovoltaic Under Harsh Climate Weather Conditions of Iraq: Baghdad Case Study.** *AIP Conference Proceedings* 2022; **2415**(1):020012,(1-12).

- [21] Gaeid KS, Uddin MN, Mohamed MK, Mohmmoud ON. **Design and Implement of Dual Axis Solar Tracker System Based Arduino.** *Tikrit Journal of Engineering Sciences* 2020; **27**(2):71–81.
- [22] Chaichan MT, Kazem HA. **Experimental Evaluation of Dust Composition Impact on Photovoltaic Performance in Iraq.** *Energy Sources, Part A: Recovery, Utilization and Environmental Effects; Informa UK Limited* 2020: p. 1-22.
- [23] Mohammed BF. **Position Control of Solar Panel Receiver by Joint Generated Power and Received Signal Power Maximization.** *Tikrit Journal of Engineering Sciences* 2018; **25**(3):24–29.
- [24] Mulyana T, Sebayang D, Fajrina F, Raihan R, Faizal M. **Design and Analysis of Solar Smartflower Simulation by Solidwork Program.** *IOP Conference Series: Materials Science and Engineering* 2018; **343**(1): 012019, (1-9).
- [25] Kiray V. **A Research Study to Increase Usage of PVs in Residential Areas.** *Frontiers in Energy Research* 2021; **9**: 680304, (1-9).
- [26] Kumar R, Bansal K, Kumar A, Yadav J, Gupta MK, Singh VK. **Renewable Energy Adoption: Design, Development, and Assessment of Solar Tree for the Mountainous Region.** *International Journal of Energy Research* 2022; **46**(2):743–759.
- [27] Zhou Z, Zhong Q. **Research on Industrial Product Design Under the Zero Carbon Concept.** *ICEMEE. E3S Web of Conferences* 2023; **406**: 03011, (1-5).
- [28] Dang DN, Le Viet T, Takano H, Duc TN. **Estimating Parameters of Photovoltaic Modules Based on Current–Voltage Characteristics at Operating Conditions.** *Energy Reports* 2023; **9**:18–26.
- [29] Nguyen-Duc T, Nguyen-Duc H, Le-Viet T, Takano H. **Single-Diode Models of PV Modules: A Comparison of Conventional Approaches and Proposal of a Novel Model.** *Energies* 2020; **13**(6): 1296, (1-22).
- [30] Sharma A, Sharma A, Averbukh M, Jately V, Azzopardi B. **An Effective Method for Parameter Estimation of a Solar Cell.** *Electronics (Switzerland)* 2021; **10**(3):1–22.
- [31] Changmai P, Deka S, Kumar S, Babu TS, Aljafari B, Nastasi B. **A Critical Review on the Estimation Techniques of the Solar PV Cell's Unknown Parameters.** *Energies* 2022; **15**(19):1-20.
- [32] Araújo N, Sousa FJP. **Equivalent Models for Photovoltaic Cell – a Review.** *Thermal Engineering Magazine* 2020; **19**(2):77–98.
- [33] Ellithy HH, Taha AM, Hasanien HM, Attia MA, El-Shahat A, Aleem SHEA. **Estimation of Parameters of Triple Diode Photovoltaic Models Using Hybrid Particle Swarm and Grey Wolf Optimization.** *Sustainability* 2022; **14**(15): 9046, (1-19).
- [34] Gruner VF, Zanotti JW, Santos WM, Pereira TA, Schmitz L, Martins DC. **Modified Current Sensorless Incremental Conductance Algorithm for Photovoltaic Systems.** *Energies* 2023; **16**(2):1-16.
- [35] Hassan O, Zakzouk N, Abdelsalam A. **Novel Photovoltaic Empirical Mathematical Model Based on Function Representation of Captured Figures from Commercial Panels Datasheet.** *Mathematics* 2022; **10**(3): 476, (1-29).
- [36] Kongphet V, Migan-Dubois A, Delpha C, Lechenadec JY, Diallo D. **Low-Cost I–V Tracer for PV Fault Diagnosis Using Single-Diode Model Parameters and I–V Curve Characteristics.** *Energies* 2022; **15**(15):1-31.
- [37] Premkumar M, Jangir P, Kumar C, Sundarsingh Jebaseelan SDT, Alhelou HH, Madurai Elavarasan R. **Constraint Estimation in Three-Diode Solar Photovoltaic Model Using Gaussian and Cauchy Mutation-Based Hunger Games Search Optimizer and Enhanced Newton–Raphson Method.** *IET Renewable Power Generation* 2022; **16**(8):1733–1772.
- [38] Zohal B, Amiry H, Yadir S, Baghaz E, Bendaoud R, El-Abidi A. **Prediction of the Performance of Photovoltaic Modules from the Behavior of Physical Parameters According to Irradiance and Temperature.** *International Journal of Intelligent Engineering and Systems* 2023; **16**(1):502–517.
- [39] Internet Source: **Smartflower. Smartflower-the world's first all-in-one solar system.** 2023. Available from:[https://www.buildersshow.com/assets/docs/ibs/pressKits/PK\\_37837\\_Smartflowerbrochure24Page.pdf](https://www.buildersshow.com/assets/docs/ibs/pressKits/PK_37837_Smartflowerbrochure24Page.pdf).